

Fatigue of continuous cast AA5754 Al alloy sheet

J. X. Li¹, X. Y. Wen³, C.-S. Man² and T. Zhai*¹

The continuous casting technology is a cost effective way to produce aluminium alloy sheet. As a result, aluminium alloys produced by this technology have great potentials to substitute steel in autobody panel applications. In the present work, fatigue tests were carried out on hot band (in as received and heat treated conditions) of a continuous cast AA 5754 aluminium alloy (4 mm thick) in directions of 0, 45 and 90° relative to the rolling direction. S–N curves of the alloy were measured in these directions. The alloy was produced using a twin belt continuous caster. The heat treatment on the alloy was conducted using both a batch anneal furnace at a slow heating rate (0.01°C s⁻¹) and an induction heater at a fast heating rate (116°C s⁻¹). The effects of heating/cooling rates during heat treatment on the fatigue anisotropy were studied in the alloy. It was found that induction heat treatment at 465°C greatly improved the tensile isotropy and reduced the fatigue anisotropy in this alloy.

Keywords: Continuous casting, Aluminium alloy, Fatigue property, Texture, Anisotropy

Introduction

Continuous casting (CC), especially twin belt continuous casting, has proved to be a cost effective way to produce commercial sheet aluminium alloys, e.g. 3000, 5000 and 6000 series, compared with the conventional direct chill (DC) ingot process.^{1–3} In twin belt continuous casting, a molten metal is directly poured into two rolling steel belts which are cooled by water to form a slab. The slab is then immediately fed into three consecutive hot rolling mills to form hot band products. In contrast, the DC process includes ingot casting, scalping, homogenisation and breakdown before hot rolling. The Al alloys produced by the CC method present significant cost savings (typically over 25% energy savings and 15% cost savings) and also possess the mechanical properties comparable to those of their DC counterparts.² They have so far demonstrated great competitiveness on the Al sheet market.

There are, however, still great differences in microstructure and mechanical properties between CC and DC Al alloys.⁴ The CC Al alloys generally contain coarser and more elongated constituent particles and show different recrystallisation characteristics, in comparison with their DC counterparts.² For example, a fully recrystallised hot band CC AA 5182 Al alloy exhibits a strong random texture and a coarse elongated grain structure, whereas a strong cube texture

and finer equiaxed grains are typically observed in the recrystallised DC AA 5182 Al alloy. It is believed that these differences between the CC and DC Al alloys are likely to be caused by higher levels of solid solution in the CC alloys and much lower plastic deformation imparted by the CC process. Hot bands of the CC AA 5182 Al alloy generally exhibits a typical deformation microstructure with a deformed grain structure and a strong β fibre texture. Its mechanical isotropy can be greatly improved by recrystallisation heat treatment.²

AA5754 Al alloys are a solid solution hardened Al–Mg alloy, offering moderate strength, and are typically used in engineering structural applications. Their sheet products are traditionally predominantly produced using the DC method. In recent years, they have been successfully produced using the twin belt continuous casting technology by Aleris International.⁵ As other Al–Mg CC alloys, they possess the overall mechanical properties that are comparable to those of their DC counterparts, although there are still certain differences in microstructure (such as grain structure and second phase particles), texture and mechanical properties between them.^{6,7} Work has recently been done on the DC AA 5754 Al alloys to study their bending,⁸ flow behaviour,⁹ fatigue performance and fracture behaviour.^{10–13} However, no work has been done on the fatigue properties of continuous cast AA 5754 Al alloys. The fatigue properties of these alloys are important to structural design, and therefore, need to be studied.¹⁴

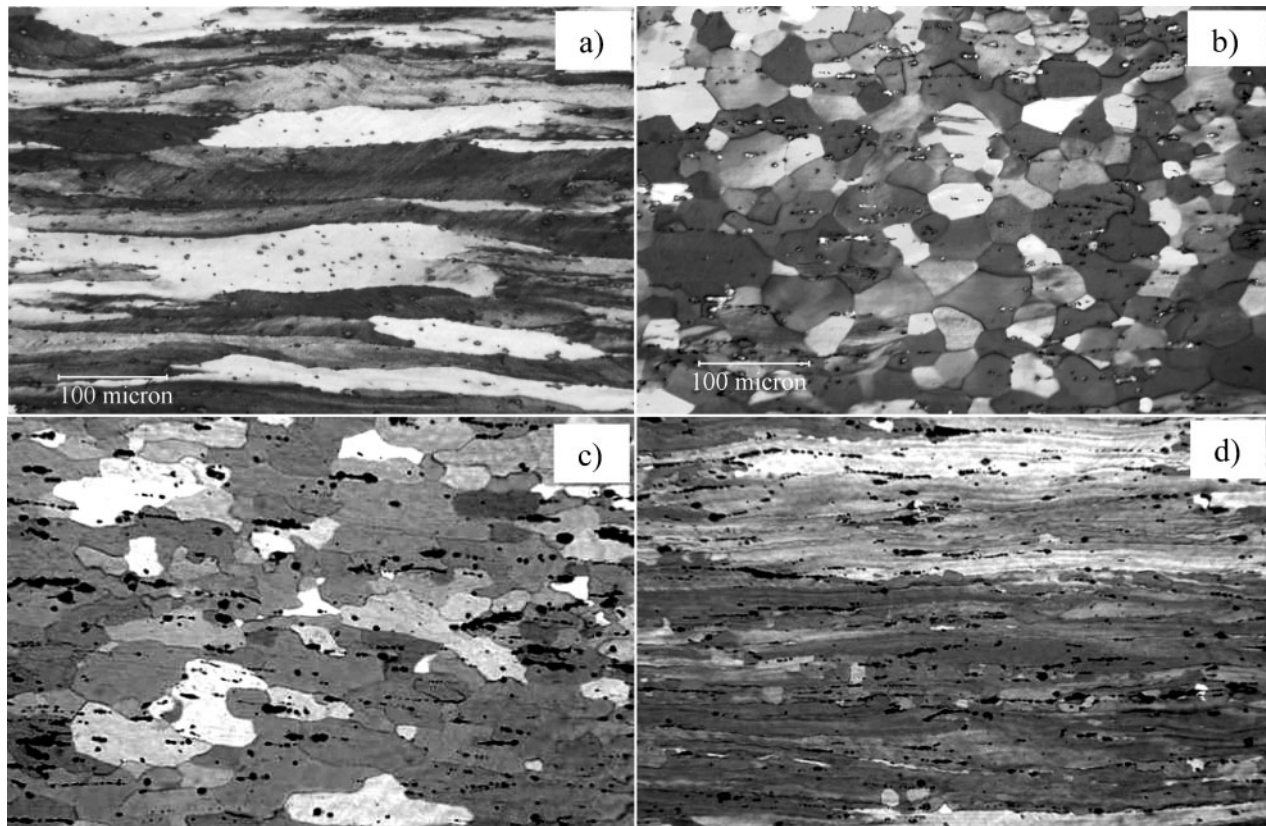
In the present work, fatigue anisotropy was studied of commercial CC 5754 Al alloys after different heat treatments. The effects of heating and cooling rates were investigated on the fatigue properties and mechanical

¹Department of Chemical and Materials Engineering, University of Kentucky, 177 F. Paul Anderson Tower, Lexington, KY 40506, USA

²Department of Mathematics, University of Kentucky, Lexington, KY 40506, USA

³Center for Aluminum Technology, University of Kentucky, 1505 Bull Lea Road, Lexington, KY 40511, USA

*Corresponding author, email tzhai@engr.uky.edu



a as produced; b annealed at 465°C by induction heating; c annealed at 400°C by batch annealing; d induction heated up to 465°C and quenched

1 Microstructures of continuous cast AA 5754 Al alloy hot bands

anisotropy in these alloys. Texture was also measured to correlate with the mechanical performance of the alloys.

Experimental procedure

The material used in the present work was a continuous cast AA 5754 Al–Mg alloy produced using a twin belt Hazlet continuous caster by Aleris International. The gauge of the alloy was 4 mm in thickness. The chemical composition of the alloy is 0.095Si–0.239Fe–0.028Cu–0.316Mn–2.854Mg–0.011Cr (wt-%). Some of the alloy had been induction heated up to 465°C in the production line at a heating rate of $\sim 116^\circ\text{C s}^{-1}$ immediately after the final hot rolling mill. It was subsequently coiled and cooled slowly in air at a rate equivalent to that in normal furnace cooling, because the coils were large, >2 m in diameter. The rest of the as received alloy was in the normal hot band condition, i.e. hot rolled products. To study the microstructure evolution, some of the induction heated samples were water quenched immediately after they reached 465°C during induction annealing. The hot band alloy was annealed at 400°C for 3 h at a slow heating rate of $0.01^\circ\text{C s}^{-1}$ and then cooled quickly in air.

Tensile specimens were prepared with a gauge length of 25.4 mm and a width of 6.35 mm. The specimens were cut along three directions (0, 45 and 90°) relative to the rolling direction. Tensile testing was performed at room temperature in air. Four samples were tested in each direction.

Fatigue specimens were also machined in the same geometry and directions as the tensile specimens. High cycle fatigue tests were conducted to measure S–N

curves on an Instron 8800 servohydraulic testing machine at room temperature and a frequency of 20 Hz in air. Tension–tension loading with a stress ratio R of 0.1 and a sinusoidal waveform were employed in these tests. The maximum loading stress was related to the yield strength. In the present study, the fatigue life was measured at a runout number between 3×10^6 and 5×10^6 cycles, rather than the commonly used 10^7 cycles.

Optical microscopy and scanning electron microscopy (SEM) were used to investigate the microstructure and the fatigue fracture surfaces of the alloy. Samples for metallographical observations were sectioned parallel to the L–S (rolling/short transverse directions) plane. With the X-ray diffraction method, $\{111\}$ $\{200\}$ $\{220\}$ pole figures were measured. Based on the data from the three pole figures, the orientation distribution function (ODF) was calculated to quantify volume fractions of texture components using the method described in Ref. 15.

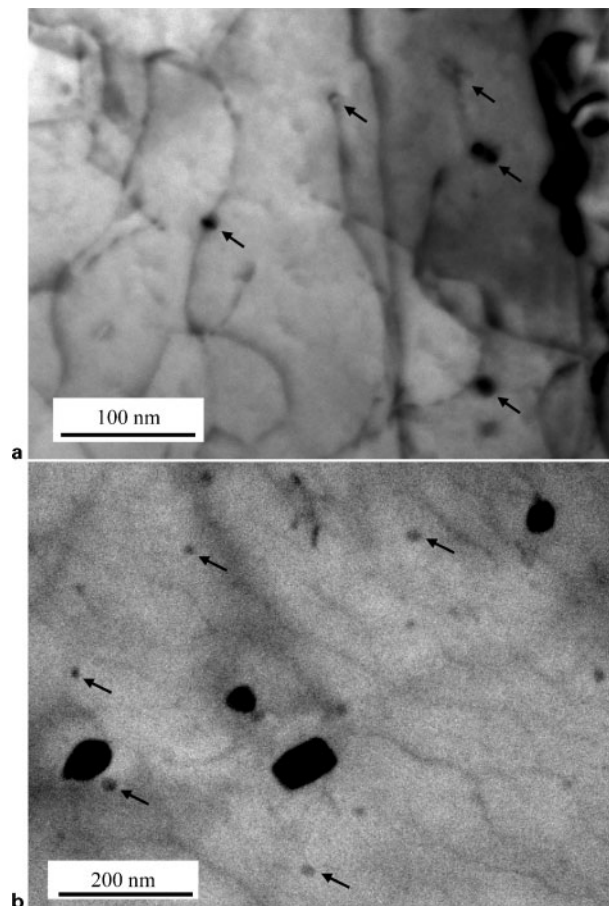
Results and discussion

Microstructure

Microstructures of hot band samples as produced, heat treated by an induction heater and a furnace, and induction heated and then water quenched are shown in Fig. 1. The as produced hot band exhibited a deformed grain structure (elongated in the rolling direction) (Fig. 1a). The grain structure was also slightly elongated in the furnace annealed hot band (Fig. 1c), but the grains were much smaller than those in the as produced hot band. As shown in Fig. 1b, after induction annealing, the hot band appeared to have a fully recrystallized grain structure, much finer, equiaxed and uniform. The

grain size was about one-third of that observed in furnace annealed samples, although the annealing temperature (465°C) was even higher than that (400°C) used in the furnace annealing. Fine, equiaxed and uniform grains have also been observed in salt bath (the heating rate is $\sim 15^\circ\text{C s}^{-1}$) annealed CC AA 5182 Al alloys.² It was likely that rapid heating gave rise to more grain nucleation sites during recrystallisation, thus resulting in the final grain structure being finer, more uniform and equiaxed in the alloy. The more the grains, the smaller the average grain size will be in an alloy. As discussed later in the present paper, the fine, uniform and equiaxed grain structure also contributed to the improved tensile isotropy of the alloy after induction annealing. The fact that the sample, which was induction heated and then water quenched, showed a partially recrystallised grain structure indicates that complete recrystallisation occurred in coils after induction heating.

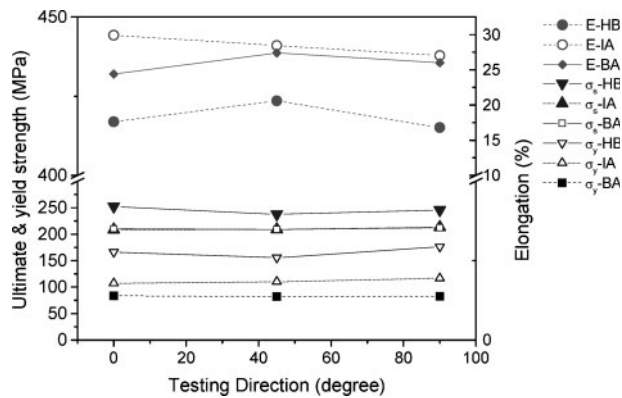
It is interesting to notice that a coarser and elongated grain structure was observed in the furnace annealed sample, in contrast to the fine equiaxed grain structure in the inline annealed sample. In induction annealing, the heating rate was very fast, $\sim 116^\circ\text{C s}^{-1}$, compared with $0.01^\circ\text{C s}^{-1}$ in batch annealing. The fast heating suppressed the recovery process and retained more stored strain energy that could drive the recrystallisation process in the 5754 alloy. Higher driving pressure for recrystallisation resulted in more grain nucleation, thus leading to the formation of fine and uniform grain structure in the sample recrystallised by induction annealing. The coarse and elongated grain structure observed in batch annealed sample was likely to be caused by precipitation taking place during heating in the furnace annealing treatment because the heating rate was so slow. Similar to CC AA 5182 Al alloys,² the as received CC AA 5754 Al alloy hot band had a high level of solid solution (supersaturated Mn, in particular), owing to a higher cooling rate in solidification and lack of homogenisation treatment in the continuous cast route. This was verified by resistivity measurement shown in Table 1, $5.145 \times 10^{-8} \Omega \text{ m}$ for the as received hot band, $5.086 \times 10^{-8} \Omega \text{ m}$ for induction heat treated samples and $5.052 \times 10^{-8} \Omega \text{ m}$ for the furnace annealed samples. Because the resistivity is directly related to the solid solution level in alloys, the as received hot band had the highest resistivity and the furnace annealed sample had the least resistivity. This indicated that more precipitation, which was likely to be $\text{Al}_6(\text{Mn,Fe})$ that precipitates between 371 and 510°C, took place during the furnace annealing than in the induction heat treatment. Figure 2 shows TEM micrographs of fine precipitates in both batch and induction annealed samples. These precipitates were often hard to detect, and analyses in TEM and more work need to be done to identify them in future. The size of these precipitates was $\sim 20 \text{ nm}$. Using a nanobeam technique, it was found that they contained Al, Mn and Fe and hence they were possibly $\text{Al}_6(\text{Mn,Fe})$. It is evident in Fig. 2a that the precipitates had more interaction with dislocations in the batch annealed sample than that (Fig. 2b) in the inline annealed sample. This may have something to do with the difference in heating rate between the two samples. Slow heating allowed precipitates to pin dislocations before they could rearrange themselves in



2 Transmission electron microscopy images showing precipitates (containing Al, Mn and Fe) in **a** batch annealed sample and **b** inline annealed sample: most precipitates in **a** interact with dislocations

the process of recrystallisation in batch annealed samples, whereas precipitates were formed only in matrix after dislocation arrangement in the inline annealed sample. The great difference in heating rate was likely to be the main cause for the observed difference in the grain structure between the batch and induction annealed samples.

It has been recognised that precipitation before and during recrystallisation profoundly influences the recrystallisation process in commercial purity Al and Al–Mn alloys.^{16–19} The concurrent precipitation promotes the formation of strong cube texture component in commercial purity Al, strong P component ($\{110\}\langle 665 \rangle$) and ND rotated cube texture in Al–Mn alloys, and strong $\{113\}\langle 110 \rangle$ in Al–Mg–Mn–Cr 5083 CC alloys. The grains formed with concurrent precipitation during recrystallisation are also coarse and elongated in the rolling direction. The concurrent precipitation at the existing high angle grain boundaries, which are predominantly along the rolling direction, pin these boundaries, making it difficult for recrystallising grains to grow in the direction perpendicular to the rolling plane. As a result, the so recrystallised grains are coarse and elongated in the rolling direction in these alloys. Furthermore, stringers of particles observed in the rolling direction might also have contributed to the formation of the elongated grains in the CC AA 5754 Al alloy. These particles provided more pinning force in the direction perpendicular to the rolling plane.^{20,21}



3 Tensile properties of as received hot band, induction annealed and batch annealed CC 5754 Al alloys

Therefore, the grains are coarse and the resultant texture in the furnace annealing is different from that without the concurrent precipitation effect in the CC AA 5754 alloy.

Tensile properties

The anisotropy of the tensile properties, such as ultimate tensile strength σ_s , yield strength $\sigma_{0.2}$ and elongation, is plotted in Fig. 3. The elongation of the alloy was significantly improved by the induction annealing, especially those values in 0 and 90° directions, from 17.6 to 29.9% and 16.8 to 27% respectively. The hot band became more isotropic within its rolling plane in terms of its tensile properties after annealing. The ultimate tensile strength was 252, 237 and 245 MPa in 0, 45 and 90° directions in the as received hot band respectively. After annealing, they were decreased to 208.6, 209 and 213 MPa respectively. In the meantime, the yield strength in these three directions were changed from 165.3, 155.6 and 176 MPa to 106.9, 110.8 and 116.3 MPa respectively. The improvement of the tensile isotropy in the hot band CC AA 5754 alloy after induction heat treatment was partially due to the formation of uniform and equiaxed grain structure in this sample.

Among the four studied conditions, the as received hot band had the highest yield strength in 0° direction (165.3 MPa), compared with 136.6 MPa for the induction annealed and water quenched sample, 106.9 MPa for the induction annealed and slowly cooled sample and 83.4 MPa for the batch annealed sample. The tensile yield strengths were correlated well with the microstructures shown in Fig. 1. The hot band with the deformed microstructure showed the highest tensile yield strength, whereas the recrystallised coarse grain structure of the batch annealed sample had the lowest tensile yield strength. Before water quenching, the inline induction annealing process was too fast to complete the recrystallisation process. Therefore, the microstructure consisted of few recrystallised grains (Fig. 1d), which

Table 1 Electrical resistivity of tested AA 5754 alloy in four conditions, $10^{-8} \Omega \text{ m}$

Samples	Resistivity
As received hot band	5.145
Induction annealed, 465°C	5.086
Induction annealed and water quenched	5.1
Batch annealed, 400°C	5.052

understandably gave rise to a higher tensile yield strength. In the inline annealed and slowly cooled sample, the grain structure was completely recrystallised but finer compared with that of the furnace annealed sample.

Compared with the tensile properties of the batch annealed sample, the induction annealed samples showed both higher yield strength and higher elongation in all three tested directions, whereas their ultimate tensile strength was almost same as that of the batch annealed samples, as shown in Fig. 3. The yield strength of the batch annealed samples was 83.4, 82 and 82.7 MPa, and the elongation 24.4, 27.4 and 26% in directions of 0, 45 and 90° respectively. The significant improvement on the tensile properties of the induction annealed samples was likely to be due to their finer and more uniform grain structure. As shown in Fig. 1, the induction annealed sample had a rather uniform grain size of $\sim 40 \mu\text{m}$, whereas the batch annealed sample showed quite non-uniform grain structure, with a size of $>110 \mu\text{m}$ in the rolling direction and $50 \mu\text{m}$ in the short transverse direction. Slightly higher levels of solid solution in the induction annealed sample than that of the batch annealed samples, as indicated by resistivity measurement (Table 1), may have also contributed to the higher yield strength in the sample. Texture might not be a factor that contributed to the difference in tensile properties between the batch and induction annealed samples, because their textures were almost identical, as shown in Table 2.

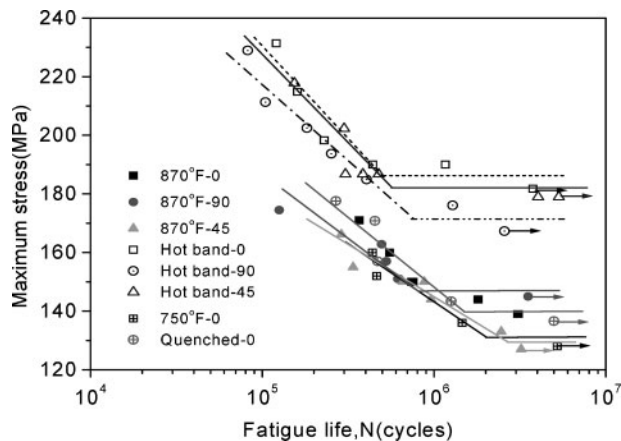
The tensile properties of the CC 5754 alloy studied in the present work were comparable to those ($\sigma_y=80 \text{ MPa min.}$, $\sigma_s=190 \text{ MPa min.}$ and elongation= $18\% \text{ min.}$) reported in the DC 5754 alloys. It is evident that the induction annealed CC alloy samples showed much better tensile properties than those of its DC counterpart.

Fatigue properties

S-N curves (stress *v.* numbers of cycles to failure) measured on the four conditions of the CC AA 5754 Al alloy are given in Figs. 4 and 5. The *y* axis is plotted with maximum stress in Fig. 4, whereas the ratio of maximum fatigue stress to tensile yield strength is employed in Fig. 5. These two values were used to reflect the absolute and relative fatigue strengths which were equally important in engineering design. Unlike most steels, aluminium alloys sometimes do not have a

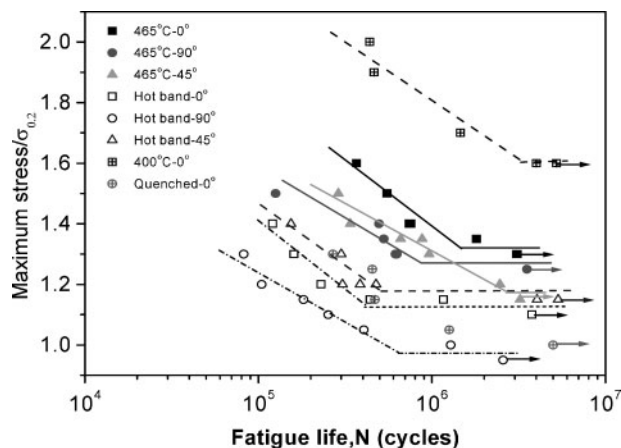
Table 2 Volume fractions of main texture components measured from central plane of CC AA 5754 Al alloys, %

	Cube	Goss	Brass	S	Copper	R cube
Hot band	1.60	4.96	21.84	28.29	12.57	0.79
Batch annealed, 400°C	8.56	3.64	7.65	8.45	3.33	3.05
Induction annealed, 465°C	8.33	3.45	6.23	7.29	3.23	4.06
Induction heated and water quenched	3.09	4.07	22.83	32.21	14.77	0.57

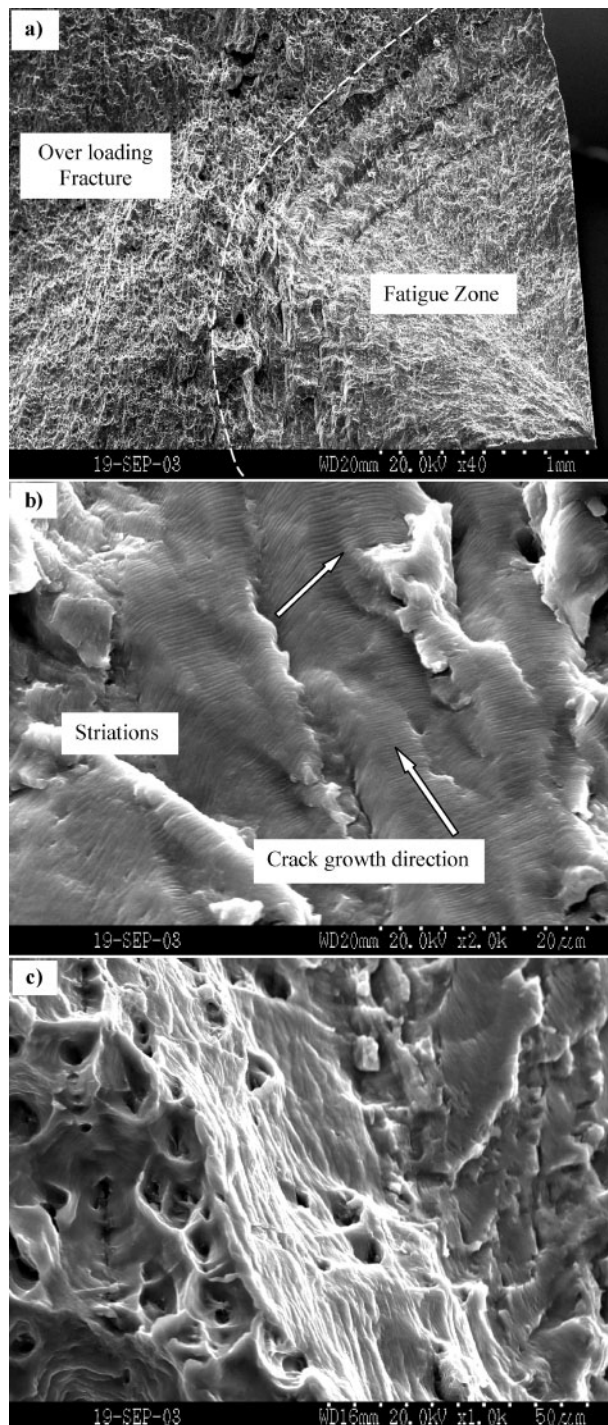


4 S-N curves for CC 5754 Al alloy with S in maximum stress

well defined fatigue limit. The fatigue limit used in the present work was defined as the maximum stress at which a sample did not fail after 3×10^6 cycles. For the CC AA 5754 Al alloy, the fatigue strength was different in three testing directions and displayed fatigue anisotropy. The sample with the highest absolute fatigue strength (182 MPa) was the as received hot band in the 0° direction. This was the direction that had the highest ultimate tensile strength (252 MPa). In the recrystallised condition, the 90° sample that was annealed at 465°C had the highest ultimate tensile strength (213 MPa). It was also found that it was the sample that had the highest relative fatigue strength (140 MPa) among all the recrystallised samples. This was in agreement with the relationship that the fatigue strength of many aluminium alloys is proportional to their ultimate tensile strength, as reported in the literature.¹² This was also true for the induction annealing and then water quenching, and the batch annealing samples which were only tested in the 0° direction. The water quenched sample has an ultimate tensile strength of 236 MPa whereas the batch annealing one 209 MPa. As shown in Fig. 4, the water quenched sample has higher fatigue strength than the batch annealing sample, and the fatigue strengths for both of them are lower than the as received hot band which has an ultimate tensile strength of 252 MPa in the 0° direction. However, the direction



5 S-N curves for CC 5754 Al alloy with S in ratio of maximum stress and yield strength

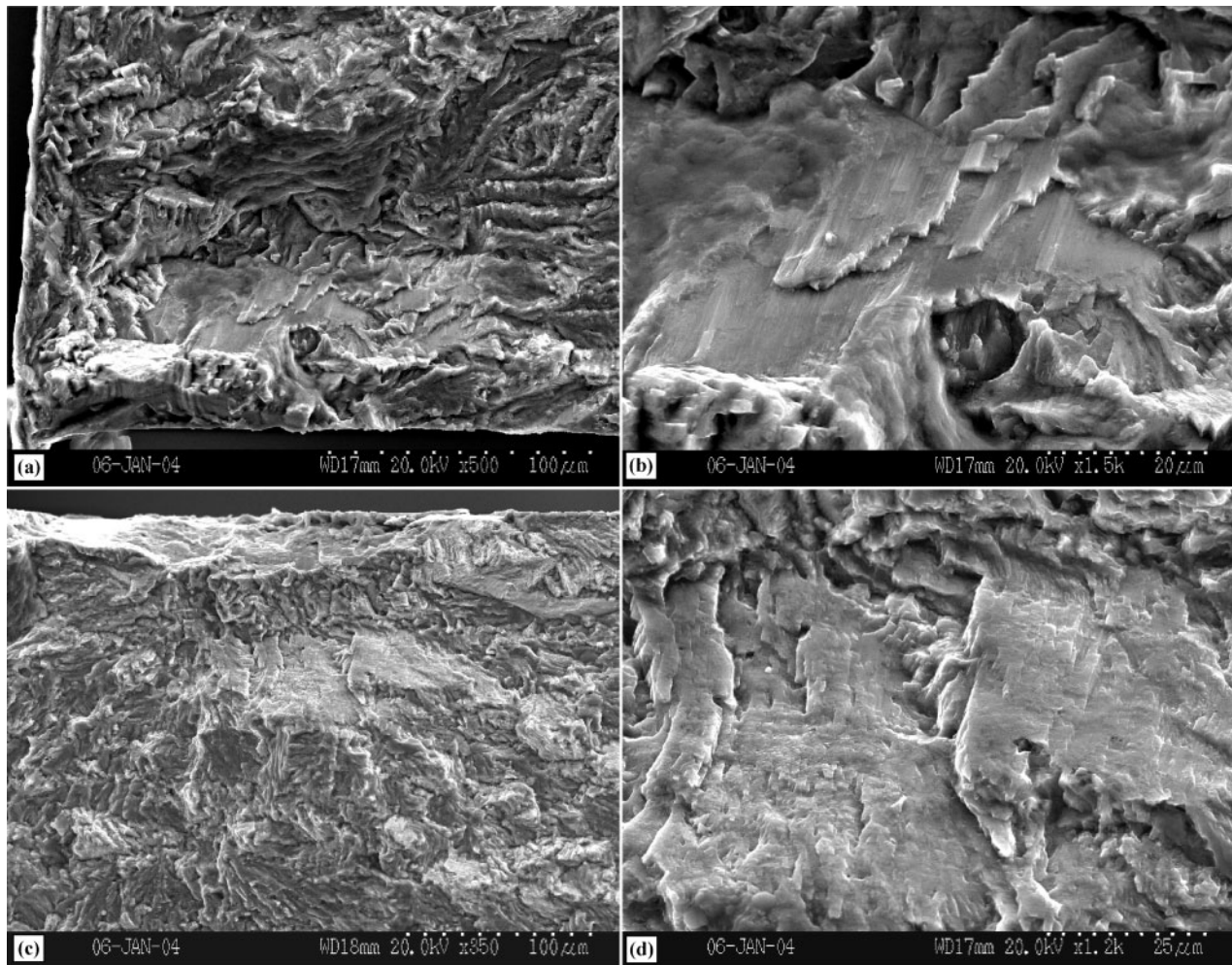


a low magnification micrograph showing crack initiation at sample corner, fatigue zone and instantaneous fracture zone; b striations in fatigue fracture zone; c transition from fatigue to instantaneous fracture

6 Scanning electron microscopy images showing fatigue fracture surface of as received hot band CC AA 5754 Al alloy (45° direction, 217 MPa and 1.5×10^5 cycles)

with the lowest fatigue strength did not correlate well with the direction that had the lowest ultimate tensile strength in the alloy.

When the relative fatigue strength was considered, it was found in Fig. 5 that it was increased in all the three tested directions after 465°C annealing. The direction with the highest relative fatigue strength is 0° relative to the rolling direction under this annealing condition. The



a,b batch annealed hot band; c,d induction heated and water quenched 5754 Al alloys

7 Crystallographic fracture in crack initiation zones

relative fatigue strength was 130% after annealing which was increased from 110% in the as received hot band. Among the three directions, the sample in 90° orientation had the largest improvement on the relative fatigue strength after 465°C annealing. The fatigue strength was increased from 95% of the yield strength in the as received hot band to 120% after annealing. The sample with less change in relative fatigue strength is in the 45° direction, from 110% in the as received hot band to 115% in annealed condition.

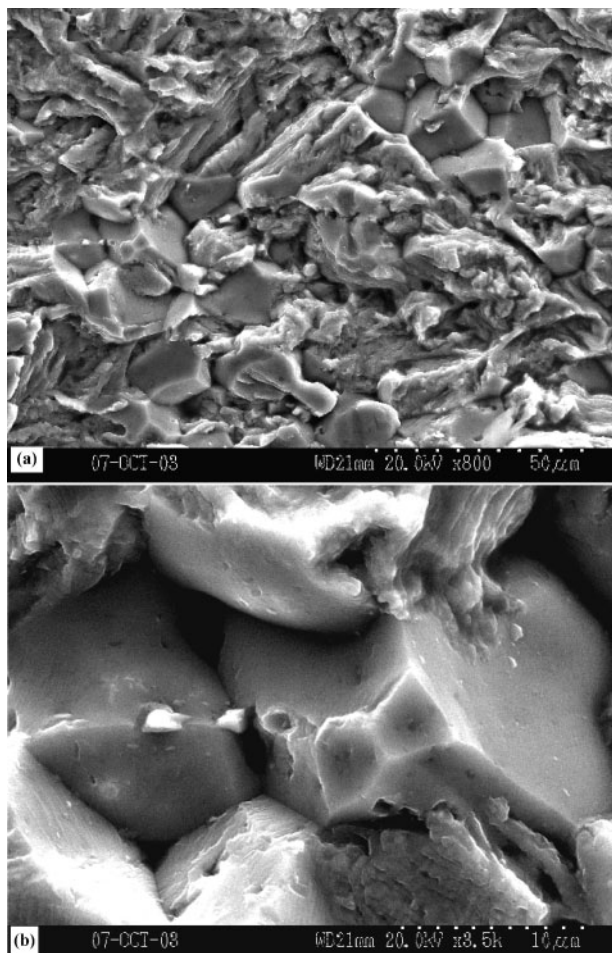
Few studies of the fatigue performance of AA 5754 Al alloys have been reported in the literature.¹⁰ The results obtained from the present work indicated that the CC AA 5754 Al alloy in an O temper condition had a fatigue limit above 120% of its $\sigma_{0.2}$. This is consistent with those of other O temper DC Al–Mg alloys.²² For example, DC AA 5052 and AA 5083 Al alloys in an O temper condition have fatigue limits of 120 and 110% of their yield strengths respectively. The fatigue behaviour of a CC AA 5083 Al alloy has recently also been investigated.²³ The fatigue limit of the CC AA 5083 alloy, after homogenisation, cold rolling (70% reduction) and annealing, is ~110% of its $\sigma_{0.2}$.

The fatigue anisotropy of this alloy was likely to be dominated by the planar arrays of coarse particles, mainly $Al_6(Fe,Mn)$, aligned in the rolling direction in the alloy. These particles were not affected by annealing treatment. The tensile anisotropy was predominantly

controlled by texture and grain structure in a sheet metal, and large second phase particles became less effective in determining the tensile anisotropy. This explains the improved tensile isotropy of the alloy after annealing, since the grains are uniform and equiaxed after anneal treatment. The fatigue properties, on the other hand, were more sensitive to local non-uniformity of plastic strain (strain concentration) and thus, they were predominantly controlled by the orientation and distribution of coarse second phase particles in the alloy. It should be understandable that the elongated particles have a minimum effect on the high cycle fatigue properties when parallel to the loading axis, whereas they have a maximum effects when aligned at either 90 or 45° relative to the rolling direction, because they could either cause more non-uniform plastic strain around these particles or fracture in these particles. This may explain the fatigue limits being relatively inferior in 45 and 90° in the as received 5754 hot band, and 45° in the 465°C annealed hot band to that in the rolling direction in this alloy.

Fatigue fractographies

The CC AA 5754 Al alloy exhibited a fatigue fracture which was, in general, similar as that in DC Al–Mg alloys.¹⁰ It was found that fatigue crack initiation was not related to large constituent particles in all the four different samples, but typically to a corner of these



8 Induction heat treated sample with intergranular fracture in a low magnification and b high magnification

specimens in all the tested directions, as shown in Fig. 6a where beach marks are visible. The sample shown in Fig. 6a was as received hot band, and failed at 1.5×10^5 cycles under a maximum stress of 217 MPa. The loading axis was along 45° relative to the rolling direction. At higher magnifications (Fig. 6b and c), striations were observed in the fatigue fracture region whereas the instantaneous fracture zone showed dimple type fracture. These striations were formed as a result of non-crystallographic growth of the fatigue crack²⁴ and can provide information about the crack growth direction and crack growth rate. According to the two models developed by McMillan/Pelloux and Laird, the formation of these striations is the result of the cyclic strain hardening effect at the crack tip.²⁵

Crystallographic cracking was also observed in the crack initiation zone in batch annealed (Fig. 7a and b) and induction heated and water quenched (Fig. 7c and d) samples. These crystallographic cracks may be related to certain types of texture in these samples, although their formation mechanism is still unclear. Intergranular fracture was also found in crack propagation zones on the fracture surface of the induction annealed, batched annealed and as received hot bands, except the induction heated and water quenched samples fatigued in all three tested directions (Fig. 8a and b). It has been reported that the intergranular fracture observed in aluminium alloys relates to segregation of Na and K at grain boundaries.^{26–28} In those cases, a Na and K content of

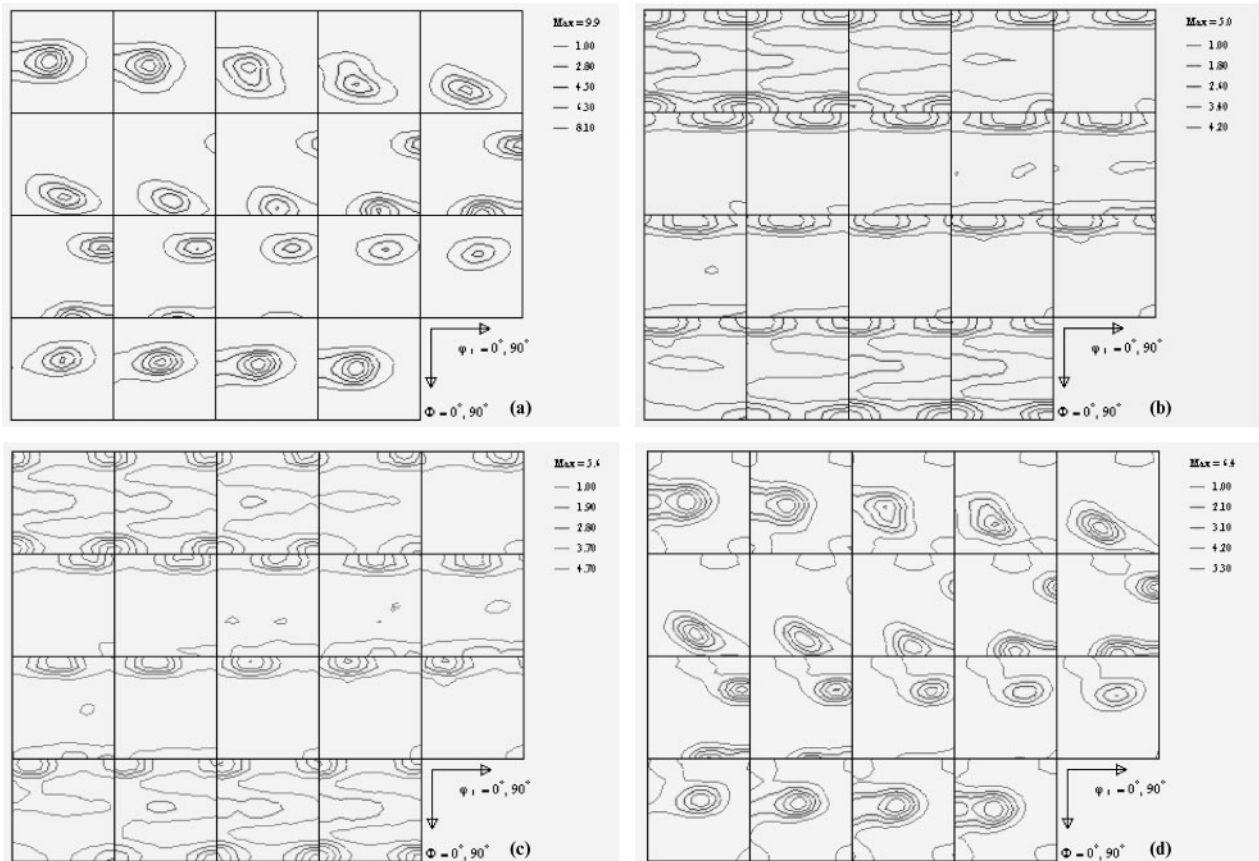
>10 ppm will cause intergranular fracture. It is likely that the intergranular fracture observed in the present work was also caused by segregation of these trace elements at grain boundaries during slow cooling of these samples, because all these three samples experienced very slow cooling after their heat treatment and no intergranular fracture was observed in the induction heated and water quenched samples. The brittle fracture can be prevented either by reducing the contents of the trace elements or by fast cooling of the alloys after heat treatment.

It is also worth mentioning that the maximum stress applied to the sample (as shown in Fig. 6a) was 140% of its yield strength. Under such a high stress level, the material still had a relatively large fatigue fracture zone which was $\sim 1/5$ of its total fracture area. This material displayed a good fatigue resistance.

Texture evolution

The orientation distribution functions (ODFs) of the as received hot band, batch annealed, induction annealed and induction heated and water quenched samples were calculated from the pole figures measured by XRD in the central planes of these samples, as shown in Fig. 9. The volume fractions of the main texture components calculated from these ODFs are listed in Table 2. It can be seen that the as received hot band had a typical rolling texture which was composed of a strong β fibre texture running from brass orientation $\{110\}\langle 112\rangle$, through S orientation $\{132\}\langle 643\rangle$, to copper orientation $\{112\}\langle 111\rangle$ (Fig. 7a). The deformation texture found in CC AA5754 hot band was consistent with the elongated deformation microstructure in this sample (Fig. 1a). After annealing, a strong cube texture (~ 8 vol.-%) was developed in both batch and induction annealed samples (Fig. 9b and c and Table 2), in addition to a rotated cube ($\{100\}\langle 011\rangle$) of about 3–4%, weak Goss ($\{110\}\langle 001\rangle$) and R component which had almost the same position as the β fibre in Euler space.^{29,30} In both of these two annealed samples, there was no noticeable difference in volume fraction of texture components. This indicated that the heating rate did not play a remarkable role in the development of texture in this alloy, although the difference in heating rate (116°C s^{-1} in the induction annealing and only $0.01^\circ\text{C s}^{-1}$ in batch annealing) was enormously large between the two heat treatments. This may be due to the fact that the inline annealed sample was heated from 260 up to 465°C at a heating rate of 116°C s^{-1} while dynamic recovery was taking place. The fast heating might not be able to preserve enough strain energy to make a noticeable effect on the development of recrystallisation texture in the sample.

The sample, which was taken right after induction annealed and quenched in water, still showed a predominant rolling texture, β fibre of 17.05%, cube 3.65% and Goss 5.88% (Table 2 and Fig. 9d). This means that the annealing duration of about 10–15 s at 465°C was not long enough for recrystallisation to take place in this sample, which was consistent with the main deformation microstructure observed in the sample (Fig. 1d). The slowly cooling after induction heating allowed completion of recrystallisation plays in this sample. In the water quenched sample, however, there was an increase in cube component, from 1.6% in the as



a as received hot band; b induction annealed sample (465°C); c batch annealed sample (400°C); d water quenched sample immediately after induction heating up to 465°C

9 Orientation distribution functions of CC AA 5754 Al alloys in central planes

received hot band to 3.09% (Table 2). This indicated that recrystallisation just started in this heat treatment, which is consistent with the microstructure observation that there were a small number of newly formed fine grains in this sample (Fig. 1d).

Conclusions

1. Continuous cast AA 5754 Al alloys had a fatigue strength of ~ 173 MPa, which was close to its yield strength in the as received hot band condition. The fatigue strength of the induction annealed hot band was ~ 130 MPa, equivalent to 120% of its yield strength, at a runout number between 3×10^6 and 5×10^6 cycles.

2. Fast induction heat treatment improved the tensile properties and their anisotropy significantly, as a result of the fine and uniform grain structure in the CC AA 5754 Al alloy.

3. In general, the fatigue limit in the rolling direction was higher than that in directions of 45 and 90° relative to the rolling direction in both the as received and induction annealed hot bands.

4. Fatigue fracture was predominantly plastic strain controlled in the as received hot band, induction annealed, batch annealed and induction heated and quenched CC AA 5754 Al alloys.

5. Intergranular fracture was observed on the fatigue fracture surfaces of the as received hot band, batch annealed, induction annealed and slowly cooled hot bands. This was likely caused by segregation of trace Na and K at grain boundaries during heat treatment in this alloy.

6. The texture consisted mainly of the β fibre component in the as received hot band CC AA 5754 Al alloy, whereas a strong cube texture was developed in the induction and batch annealed samples. The coiling and slowly cooling operation after induction heating played an important role in the recrystallisation process.

Acknowledgements

The present work is partially funded by Kentucky Science and Engineering Foundation under the contract no. KSEF-148-502-02-19. The authors would like to thank Alaris Inc. for the provision of the CC AA 5754 Al alloys for the present study and to Dr E. A. Kenik for conducting the TEM work at the Oak Ridge National Laboratory SHaRE User Center which was sponsored by the US Department of Energy, Office of Energy Efficiency and Renewable Energy, Industrial Technologies Program, Industrial Materials for the Future and the Division of Materials Sciences and Engineering, under contract DE-AC05-00OR22725 with U.T. Battelle, LLC.

References

1. S. Platek: Proc. 128th Annual Meeting Light metals '99, San Diego, CA, USA, 28 February–4 March 1999, TMS, 939–944.
2. X. F. Yu, Y. M. Zhao, X. Y. Wen and T. Zhai: *Mater. Sci. Eng. A*, 2005, **A394**, (1–2), 376–384.
3. W. C. Liu, T. Zhai and J. G. Morris: *Scr. Mater.*, 2004, **51**, (2), 83–88.
4. M. Gallerneault and D. Lloyd: *Metall. Ital.*, 2002, **94**, (1), 15–18.
5. Z. Li, S. Kirkland, S. X. Ding and P. Platek: *JOM*, 2004, **56**, (11), 287.

6. P. A. Friedman and A. M. Sherman: in 'Automotive alloy II', (ed. S. K. Das), 147–160; 1998, San Antonio, TX, TMS.
7. M. Gallerneault and D. Lloyd: *Mater. Sci. Forum*, 2002, **396–402**, 95–100.
8. D. J. Lloyd, D. Evans, C. Pelow, P. Nolan and M. Jain: *Mater. Sci. Technol.*, 2002, **18**, (6), 621–628.
9. M. C. Butuc, J. J. Grácio, J. Ferreira Duarte and A. Barata da Rocha: Proc. Cong. IDDRG '98, Brussels, Belgium, June 1998, IDDRG, 489–496.
10. A. A. Luo, R. C. Kubic and J. M. Tartaglia: *Metall. Mater. Trans. A*, 2003, **34A**, (11), 2549–2557.
11. K. Spencer, S. F. Corbin and D. J. Lloyd: *Mater. Sci. Eng. A*, 2002, **A322**, 81–90.
12. J. L. Gimple, D. S. Wilkinson, J. D. Embury and J. J. Lewandowski: in 'Aluminum 2001: proceedings of the TMS 2001', (ed. S. K. Das *et al.*), 17–29; 2001, Warrendale, PA, TMS.
13. C. B. Fuller, A. R. Krause, D. C. Dunand and D. N. Seidman: *Mater. Sci. Eng. A*, 2002, **A338**, 8–16.
14. S. Suresh: 'Fatigue of materials', 17; 2001, Cambridge, Cambridge University Press.
15. X. Y. Wen, W. C. Liu, T. Zhai, J. Liu, X. M. Cheng, S. K. Das and J. G. Morris: Proc. Symp. on 'Automotive alloys and aluminum sheet and plate rolling and finishing technology', Seattle, WA, USA, February 2002, TMS, 219–228.
16. J. A. Saeter and E. Nes: *Mater. Sci. Forum*, 1998, **273–275**, 477–482.
17. M. Somerday and F. J. Humphreys: *Mater. Sci. Forum*, 2000, **331–337**, 703–714.
18. K. Sjolstad, O. Engler, S. Tangen, K. Marthinsen and E. Nes: *Mater. Sci. Forum*, 2002, **408–412**, 1471–1476.
19. J. Li, W. C. Liu, T. Zhai and E. A. Kenik: *Scr. Mater.*, 2004, **52**, (3), 163–168.
20. E. Nes, N. Ryum and O. Hunderi: *Acta Metall.*, 1985, **33**, 11.
21. F. J. Humphreys and M. Hatherly: 'Recrystallization and related annealing phenomena', 2nd edn; 2004, Oxford, Elsevier.
22. 'Metals handbook', Vol. 19; 1998, Materials Park, OH, ASM International.
23. J. Li, J. X. Li and T. Zhai: to be submitted to *Mater. Sci. Eng. A*.
24. N. S. Stoloff and D. J. Duquette: *CRC Crit. Rev. Solid State Sci.*, Sep. 1974, 615–687.
25. J. Schijve: 'Fatigue of structures and materials'; 2001, Dordrecht, Kluwer Academic Publisher.
26. T. Zhai, A. J. Wilkinson and J. W. Martin: *Mater. Sci. Forum*, 2000, **331–337**, 1549.
27. K. T. Venkateswara Rao, R. S. Piascik, R. P. Gangloff and R. O. Ritchie: Proc. 5th Conf. on 'Al-Li alloys', (ed. T. H. Sanders, Jr and E. A. Starke, Jr), 955; 1989, Birmingham, UK, MCEP.
28. D. N. Fager, M. V. Hyatt and H. T. Diep: *Scr. Metall.*, 1986, **20**, 1159.
29. J. Hirsch and K. Lucke: *Acta Metall.*, 1985, **33**, 1927–1938.
30. W. C. Liu, T. Zhai and J. G. Morris: *Mater. Sci. Eng. A*, 2003, **A358**, 84–93.